Experiment based modeling of the mechanical expansion of tubes for the construction of heat exchangers

Available online at www.sciencedirect.com

ScienceDirect

Procedia Structural Integrity 12 (2018) 130–144

Structural Integrity Procedia

www.elsevier.com/locate/procedia

AIAS 2018 International Conference on Stress Analysis

Experiment based modeling of the mechanical expansion of tubes for the construction of heat exchangers

Massimiliano Avalle[a] *, Alessandro Scattina[b]

[a] *Università degli Studi di Genova, Via all'Opera Pia 15, 16145 Genova, Italy*
[b] *Politecnico di Torino, Corso Duca degli Abruzzi 24, 10129 Torino, Italy*

Abstract

Tube heat exchangers are made by assembling metals tubes, which the fluid to be refrigerated is passed through, with fins where a refrigerating fluid (usually air) is flown over. The heat exchange between tubes and fins is obtained by exploiting their tight contact. This necessary very tight contact is obtained by means of brazing (typically in smaller equipment) or through the forced expansion of the tubes into the fins holes. The forced expansion can be hydraulic (by some fluid put in pressure in the assembly operation) or mechanic through the insertion of a sphere or an ogive with external diameter slightly larger than the internal diameter of the tube. The sphere or the ogive is pushed along the entire length of the tube so that the tube remains plastically forced into the fins holes. The process is then repeated for all the tubes of the heat exchanger.
The present work concentrates on the mechanical expansion: to optimize the construction process it is necessary to have a model able to describe the mechanical phenomenon: that is, to evaluate the stress state in the tube during the insertion of the ogive, the residual stresses after the sphere/ogive passage, and the force required depending on the process and materials parameters (including the geometry of the tube, ogive, and fins, their material properties, friction, insertion speed etc.).
The present work will describe an analytical model able to describe the process with a good level of predictability showing the effect of the main parameters involved in the process. The model is based and validated by means of experimental tests and numerical simulations at different levels and in different conditions and materials.

Keywords: tube expansion process; analytical model; parametric analysis

* Corresponding author. Tel.: +39-010-3532241; fax: +39-010-3532834.
E-mail address: massimiliano.avalle@unige.it

10.1016/j.prostr.2018.11.100

1. Introduction

Tube heat exchangers are made by assembling metals tubes, which the fluid to be refrigerated is passed through, with fins where a refrigerating fluid (usually air) is flown over, see Thulukkanam (2000) and Schlünder (1983). The tubes are then fixed to a pair of head plates supporting the whole structure. The heat exchange is obtained by exploiting the tight contact between tubes and fins. The contact is obtained by means of brazing (typically in smaller equipment) or through the expansion of the tubes and the forced expansion into the fins holes. Expansion, as illustrated in Fig. 1, can be hydraulic (by some fluid put in pressure in the assembly operation) or mechanical through the insertion of a sphere or an ogive of external diameter slightly greater than the internal diameter of the tube. The sphere or ogive is pushed along the entire length of the tube mechanically or hydraulically so that the tube remains plastically forced into the fins holes. The process is then repeated for all the tubes of the heat exchanger. The materials involved in the process are typically stainless or carbon steel, copper-nickel alloys and titanium for the tubes, and aluminum or the copper for the fins.

Previous analytical models were developed by many authors, as summarized by Nadai (1950). In recent years, the analytical model developed by Karrech and Seibi (2010) allows the prediction of the driving force, the dissipated energy and the ogive angle, and it was validated by finite element analysis: they also propose some optimal geometry. Almeida et al. (2006) refreshed and extended the fundamentals of tube expansion and reduction using a die, by means of comprehensive theoretical and experimental investigation. They defined the formability limits of this process: ductile fracture, local buckling and wrinkling. Tang et al. (2008) proposed a complete study of the expansion process where a thick-walled microgroove copper tube is joined to aluminum fins. The results indicate that thermal–mechanical performance is mainly influenced by the expanding ratio. Tang et al. (2009) and (2011b) conducted FEM analysis, supported by experimental investigations, to study the effect of groove shape on forming quality. The outcome shows that the groove height reduction is heavily affected by the helix angle whereas the joining status between the tubes and the fins is mainly influenced by the expanding ratio. The same approach was used by Alves et al. (2006) to study the influence of the process parameters on the formability limits due to ductile fracture and wrinkling. The influence of the expansion parameters on the stress levels was studied by Seibi et al. (2011) for aluminum and steel tubes examining expansion forces and the spring back phenomenon. Tang et al. (2011) developed an FE model to improve the tube–fin contact of heat exchangers. The FE method was also used to investigate a real tube sheet fracture, as proposed by Li et al. (2010). FEM simulation and experimental data were used by Yang et al. (2010) to study the absorption behavior of the plastic energy of tubes made of aluminum and subjected to the expansion. The expansion was made with the application of an axial compression and with the use of a conical-cylindrical die.

In this overview, the goal of this study is the analysis, with an analytical model, of experimental and numerical data on the expansion process of stainless steel and titanium tubes. The developed analytical model was also used to study similar results for tubes made of copper-nickel alloys proposed by the authors in previous work, see Avalle et al. (2014), Avalle and Scattina (2012), Scattina (2016). Moreover, a parametric analysis on the main parameters of the manufacturing process was proposed. In more details, in section 2 the details about the materials investigated and the numerical simulations carried out are provided. Section 3 deals with the analytical model of the mechanical expansion process. In section 4 the results of the experimental results are compared with the results obtained with the models. In section 5 the parametric analysis is developed.

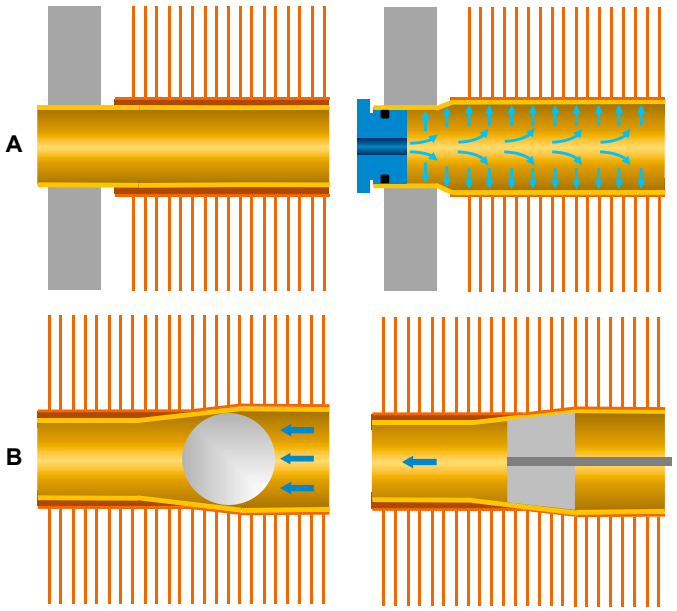

Fig. 1. Schematic of the expansion processes used for the assembly of the heat exchanger: (A) hydraulic expansion; (B) mechanical expansion obtained through the insertion of a sphere pushed by applied pressure (left) or through an ogive pushed/pulled by a rod (right).

Nomenclature

α	average slope of the ogive
d	generic diameter ($d_i \leq d \leq d_e$)
β	ratio of the internal over the external diameter of the tube (d_i / d_e)
D	nominal (external) diameter of the tube
d_i	internal diameter of the tube
d_e	external diameter of the tube
d_ogive	diameter (external) of the ogive
E	elastic modulus of the material of the tube
E_y	plastic (hardening) modulus of the material of the tube
f	friction coefficient in the process between tube and ogive
φ	friction angle
i	diametral interference ($d_{ogive} - d_i$)
p_a	axial force per unit area during insertion
p_r	radial force per unit area during insertion, internal pressure exchanged during insertion
S_y	yield strength of the material of the tube
t	initial thickness of the tube
u	generic radial displacement

2. Materials

The two main components of the heat exchangers are the tubes and the fins. The material for the fins is typically an aluminum alloy due to its characteristics of elevated heat conduction, workability, and lightweight. The tubes can

be made of different materials including copper alloys, stainless steels and titanium. In this work, the material for the fins was the aluminum alloy 8006 whereas the materials of the tubes were:

- Copper-Nickel alloy CuNi 90-10 (cupronickel)
- Stainless steel AISI 316
- Titanium alloy ASME SB338

Tensile tests were carried out on these three types of materials to get material properties. The information obtained in this phase were used for the development of the finite element (FE) models described in the following.

The experimental tests were performed by means of an Instron 8801 hydraulic universal material testing machine, located in the laboratory of the Department of Mechanics and Aerospace Engineer of the Politecnico di Torino. It is a 100 kN maximum load testing machine. The tensile tests on the tubes were performed in accordance with the ASTM E8M-98 standard. The tests on the aluminum were performed on rectangular strips cut from larger sheet. The length L of the tube specimens was 208-210 mm. For the cupronickel two values of the wall thickness t (1.0 e 1.5 mm) were considered. For the stainless steel, different types of specimen were examined as follow:

- 2 different external diameters D
- 4 different wall thicknesses t

The values of the geometrical parameters of the tube specimens considered in the experimental tests are summarized in Table 1.

Table 1. Geometrical parameters of the tube specimens considered in this work for the three analyzed materials.

		Cupronickel	*Stainless steel*		*Titanium alloy*
		External diameter D (mm)			
		15.875	15.875	19.05	19.05
Wall thickness t (mm)	1	✓	✓	✓	✓
	1.25	-	✓	-	-
	1.5	✓	-	✓	-
	1.65	-	✓	✓	-

The tests were performed in displacement control. Three loading speeds v were applied:

- 0.1 mm/s
- 5 mm/s
- 100 mm/s

The three values of the velocity were chosen in order to cover the examined range with a widely and uniform spacing considering that the strain-rate effects are usually of logarithmic nature.

Tests were conducted to bring the samples up to complete failure in traction. During the tests, samples of time, actuator stroke, load, and strain were measured (at constant time intervals). The results of the tensile tests on the tube specimens are summarized in terms of (quasi-static) stress-strain curves in Fig. 2. The reported curves are the average curves identified using a finite element model (Fig. 3). The FE software LS-DYNA was used for the simulation of the tensile tests. The implicit version of the release R7 of the software was adopted. The tube was simulated using two-dimensional shell elements with axisymmetric properties thanks to the geometry of the specimens. The average mesh size was set to 0.125°mm in order to have a significant number of elements along the tube thickness. An elastic-viscoplastic material model (name of the material card: *MAT_ELASTIC_VISCOPLASTIC_THERMAL) was adopted. The same boundary conditions applied in the experimental tests were applied in the numerical model. An inverse method process was used to obtain the parameters of the material card.

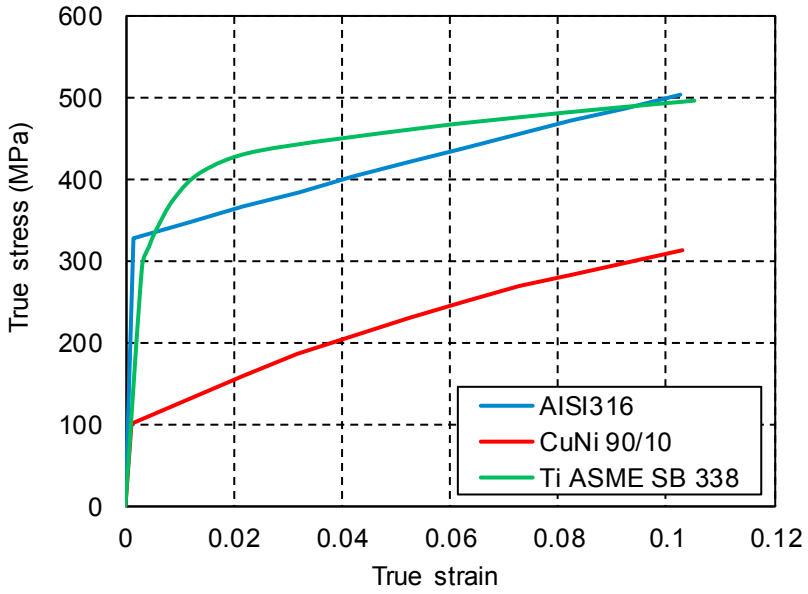

Fig. 2. Average curves of the examined materials identified with the material card *MAT_ELASTIC_VISCOPLASTIC_THERMAL in the numerical simulations developed with LS-DYNA.

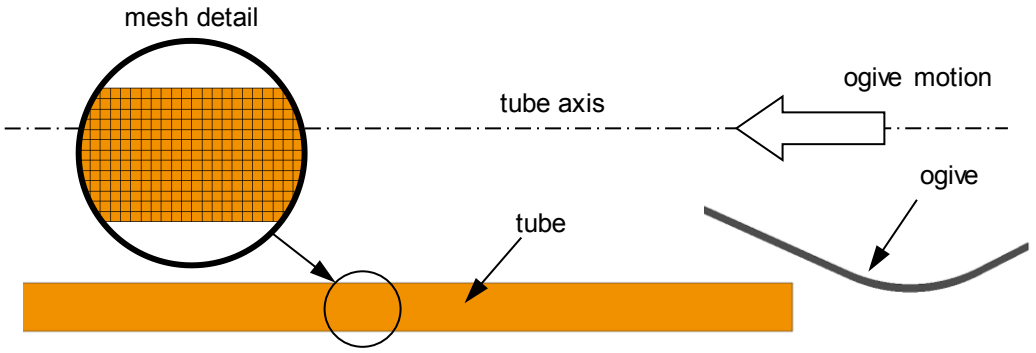

Fig. 3. Finite element model used for the study of the expansion process developed in LS-DYNA. It is a plane axisymmetric model, therefore the components appear as in a section view. Analytical model of the mechanical expansion process

3. Analytical model of the mechanical expansion process

The mechanical expansion process was studied in some previous papers, in particular with the analytical model developed by Karrech and Seibi (2010).

A simpler model is presented here. In practice it models the expansion process as the insertion of a conical ogive into the tube (Fig. 4) where the axial insertion force can be evaluated in terms of the simple equilibrium taking into account the friction f, equivalently to the equilibrium in the motion on a surface of slope α. The expression used to evaluate the axial force per unit area related to the radial pressure exerted on the inner surface of the tube is simply:

$$p_a = p_r \tan(\alpha + \varphi) = p_r \frac{f + \tan\alpha}{1 - f\tan\alpha} \qquad (1)$$

Where the friction angle φ is related to the coefficient of friction by the usual relation $f = \tan(\varphi)$.

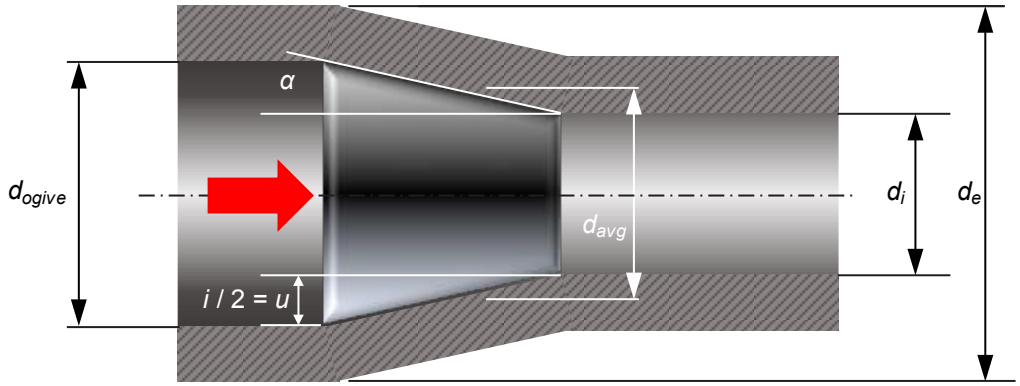

Fig. 4. Schematic representation of the expansion process for the development of the analytical model.

The axial drawing force, or axial expansion force, is then:

$$F = p_a A = p_r \tan(\alpha+\varphi)\frac{\pi}{4}\left(d_{\text{ogive}}^2 - d_{\text{i}}^2\right) = p_r \frac{f+\tan\alpha}{1-f\tan\alpha}\frac{\pi}{4}\left(d_{\text{ogive}}^2 - d_{\text{i}}^2\right) = \\ = p_r \tan(\alpha+\varphi)\frac{\pi}{4} d_i\left(d_i + 2i\right) = p_r \frac{f+\tan\alpha}{1-f\tan\alpha}\frac{\pi}{4} i\left(2d_i + i\right) \tag{2}$$

For small values of the wall thickness, Eq. (2) can be simplified as:

$$F = p_a A \approx p_r \tan(\alpha+\varphi)\frac{\pi}{2} i d_{avg} \approx p_r \frac{f+\tan\alpha}{1-f\tan\alpha}\frac{\pi}{2} i d_{avg} \tag{2a}$$

The error between the results obtained with equation (2) and those obtained with equations (2a) is less than 5% when the ratio of the thickness over the internal diameter is less than 1/10: so, Eq. (2a) can be a good approximation in many cases.

Thus, it is necessary to evaluate the internal pressure needed to expand the tube from a value of the internal diameter d_i to the value of the ogive diameter d_{ogive}: in other terms, to apply a radial displacement u at the internal diameter equal to half the interference $i = d_{ogive} - d_i$.

There are many elasto-plastic approaches for the axisymmetric solid subject to internal pressure (or alternatively to an internal radial displacement). In many cases a numerical solution is required, some analytical models give an explicit solution. For example, a solution of the problem with an elastic-perfectly plastic material was given by Nadai (1950). Fig. 5 shows a comparison between the results obtained with the Nadai analytical model and the results obtained with a numerical simulation performed with Ansys. The FE model developed in this stage was a plane model with axisymmetric elements. A non-linear simulation with the implicit version of the software (ANSYS R17.2) was performed. Ten elements were applied along the wall thickness of the tube in order to have a mesh with regular shape. Elements with similar size were also used for the modelling of the ogive. The tube was simulated using an ideal elastic-plastic material model whereas for the ogive a material model with elastic-linear properties was adopted. The standard value of the elastic modulus for a common steel was used for the material card of the ogive. The strain-rate effects were not considered in this phase for both materials. The standard algorithm of contact provided by the software used for the simulation was applied between the external surface of the ogive and the inner part of the tube. A motion law with constant velocity was applied to the ogive, whereas the constraints were applied to the tube.

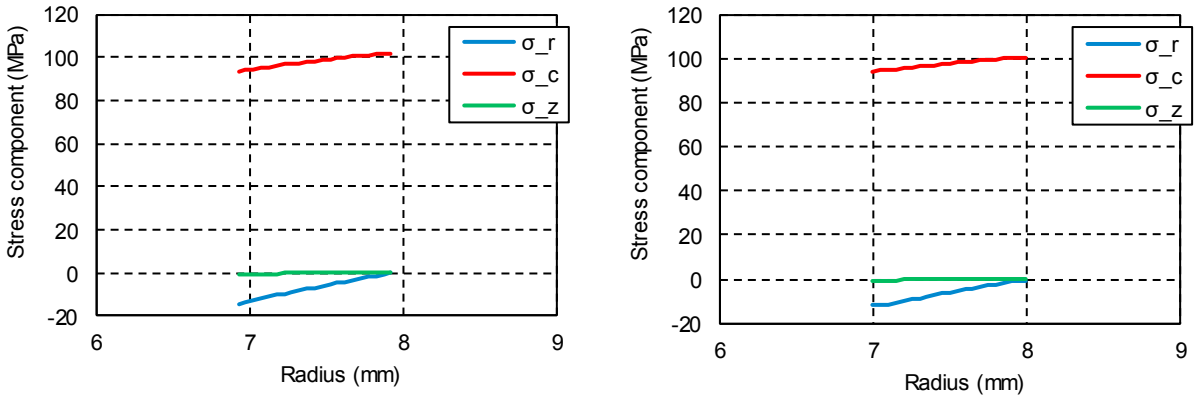

Fig. 5. Comparison of the results in the numerical simulation of the elastic-perfectly plastic materials obtained with ANSYS (left) and the Nadai analytical model (right).

In this work, a simpler solution is proposed considering the solution of the rigid-perfectly plastic material plus a solution for a rigid-linearly hardening material.

The stress state for the rigid-perfectly plastic material comes from the solution of the equation of equilibrium considering the hoop stress equal to the value of the yield strength when the axisymmetric solid is fully yielded:

$$\sigma_r = p_i \frac{d_i}{d_i - d_e}\left(\frac{d_e}{d} - 1\right) \quad \rightarrow \quad \sigma_{ri} = \sigma_r\left(d = d_i\right) = -p_i$$
$$\sigma_c = -p_i \frac{d_i}{d_i - d_e} = S_y \quad \rightarrow \quad p_i = S_y\left(\frac{d_e}{d_i} - 1\right) \tag{3}$$

The second contribution is related to the rigid-linearly hardening material, for which the stress distribution can be considered as:

$$\sigma_r = -p_i\left(\frac{d_i}{d}\right)^2\left(\frac{d_e^2 - d^2}{d_e^2 - d_i^2}\right)$$
$$\sigma_c = p_i\left(\frac{d_i}{d}\right)^2\left(\frac{d_e^2 + d^2}{d_e^2 - d_i^2}\right) \tag{4}$$
$$u_i = u\left(d = d_i\right) = p_i \frac{d_i}{2E_y}\left(\frac{d_e^2 + d^2}{d_e^2 - d_i^2} + \frac{1}{2}\right) \quad \rightarrow \quad p_i = u_i \frac{2E_y}{d_i}\frac{1}{\frac{d_e^2 + d^2}{d_e^2 - d_i^2} + \frac{1}{2}}$$

It is then possible to relate the internal pressure due to a given interference $d_{ogive} - d_i$ as follows:

$$p_r = S_y\left(\frac{1}{\beta} - 1\right) + E_y\left(\frac{i}{d_i}\right)\frac{1}{\frac{1+\beta^2}{1-\beta^2} + \frac{1}{2}} = S_y\left(\frac{d_e}{d_i} - 1\right) + E_y\left(\frac{i}{d_i}\right)\frac{1}{\frac{d_e^2 + d_i^2}{d_e^2 - d_i^2} + \frac{1}{2}} =$$
$$= S_y\left(\frac{t}{r_i}\right) + E_y\left(\frac{i}{2r_i}\right)\frac{1}{\frac{\left(1 + t/r_i\right)^2 + 1}{\left(1 + t/r_i\right)^2 - 1} + \frac{1}{2}} = S_y\left(\frac{2t}{d_i}\right) + E_y\left(\frac{i}{d_i}\right)\frac{1}{\frac{\left(1 + 2t/d_i\right)^2 + 1}{\left(1 + 2t/d_i\right)^2 - 1} + \frac{1}{2}} \tag{5}$$

Or, in a simpler form:

$$p_r = S_y\left(\frac{1}{\beta}-1\right)+E_y\left(\frac{i}{d_i}\right)\frac{2\left(1-\beta^2\right)}{3+\beta^2} = S_y\left(\frac{d_e}{d_i}-1\right)+E_y\left(\frac{i}{d_i}\right)\frac{2\left(1+\frac{d_i}{d_e}\right)\left(1-\frac{d_i}{d_e}\right)}{3+\left(\frac{d_i}{d_e}\right)^2} = \tag{5a}$$

$$= S_y\left(\frac{2t}{d_i}\right)+E_y\left(\frac{i}{d_i}\right)\frac{2\left(\frac{t}{d_i}\right)\left(1+\frac{t}{d_i}\right)}{1+3\left(\frac{t}{d_i}\right)+3\left(\frac{t}{d_i}\right)^2}$$

Eq. 5 clearly shows the main influences on the pressure and, consequently on the drawing force:

- Both yield strength and strain hardening have a linear influence
- The thickness has essentially a parabolic influence

From Eq. 2 it is also clear that friction and the shape of the ogive plays an important role on the value of the drawing force.

4. Experimental results and comparison

4.1. Experimental setup

Expansion tests were performed in two specimen configurations:

- Simple (free) tube
- Tube positioned in a simple heat-exchanger model

The heat exchanger model was a scaled down system made by assembling the fins with a six-tube hexagonal array with the tube subjected to the expansion test positioned in the geometrical center of the hexagon. The use of this assembly was more representative of the production method. The heat-exchanger model is shown in Fig. 6b. The expansion tests were done according to the pattern shown in Fig. 6a using the same testing machine described above. The test machine had two grips, one it is fixed whereas the other one is fixed on the hydraulic actuator. The tube subjected to the expansion test was constrained in the fixed grip. An ogive was fixed on a rod clamped in the grip fixed to the hydraulic actuator. The expansion was made by the motion of the hydraulic actuator which pushed the ogive inside the tube. During the expansion tests, the stroke of the hydraulic actuator and therefore of the ogive inside the tube and the force exerted by the ogive on the tube along the tube axis were recorded. In the following, this force is considered as the expansion force. The expansion tests were carried out considering two expansion velocities: $v = 10$ mm/s and $v = 100$ mm/s. The second value of the velocity is representative of the expansion velocity used in the production process. Therefore, the both values of the velocity were used for the tests on the simple tube, whereas only the highest value was used for the tests on the heat-exchanger model. The expansion tests were repeated at least three times for each considered configurations. Some grease was applied on the surface of the ogive before each test as it is done in the common production process.

The development of the analytical model discussed in this work was focused, as first step, on the expansion of the simple tube. The main amount of the expansion force was due to the deformation of the tube, whereas the amount of the material deformed on the fins was much lower. Moreover, the deformation of the fin neck is a consequence of the expansion of the tube, hence it can be considered as a second step of the process. Therefore, it is necessary to develop first a valid analytical model for the expansion of the simple tube, before to approach to the expansion of the tube on the fins. At this stage, the study of the whole expansion process needs too high simplification hypothesis.

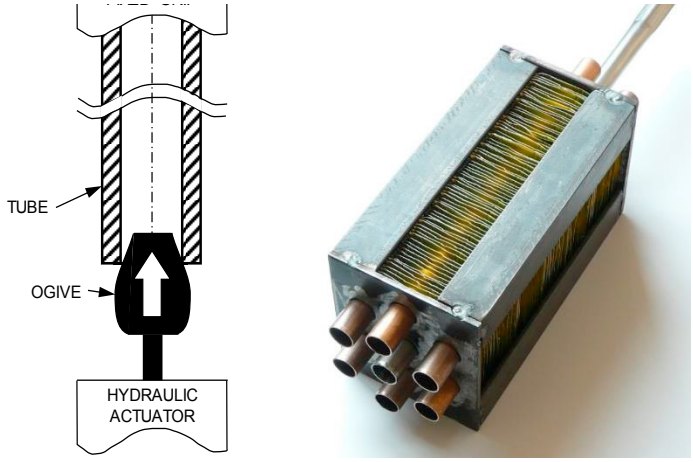

Fig. 6. Schematic of the experimental tests: (a) simple tube expansion; (b) heat-exchanger model used for some experimental tests.

4.2. Cupronickel Cu/Ni 90/10 alloy

It is a well-known and widely used material for this application. Experimental results, together with a numerical model, were previously presented by Avalle et al. (2014), Avalle and Scattina (2012) and Scattina (2016). The numerical model was obtained from that described in section §2 introducing the ogive. The ogive was simulated with the same type of elements used for the tube. A material model with rigid properties was applied to the ogive. The boundary conditions were applied as in the real process of expansion. The material is highly workable in several tube sizes and it is adaptable to many situations. Since it is the most interesting material, a lot of testing was performed in several loading conditions as described before.

The tubes were affected by geometrical irregularities: the tube axis was not exactly straight, and the tube cross-section was not perfectly constant. For this reason, the tubes showed some bending during the expansion tests. However, the tubes did not show instability during the expansion and the tests were very repeatable in all the considered configurations: the expansion force was sufficiently constant during the tests on the simple tubes. An increase in the expansion force was observed in the tests on the heat-exchanger model. This trend was due to the packaging of the fins during the expansion.

4.3. Stainless steel AISI 316

AISI 316 it is one of the mostly known stainless steel, also used in some applications where higher temperature and pressure are required.

Apart from the material characterization, tests on this material were mostly restricted to the simple tube expansion. Only some few tests were performed with the simple heat-exchanger model and will not be presented here.

The tests regarding the simple tube expansion in terms of expansion force as a function of the ogive stroke are reported in Fig. 7 in four of the six configurations reported in Table 1. Some tests had to be discarded due to an unpredictable highly irregular response. In the other tests, the measured load was quite constant. The repeatability of tests was quite high for the two intermediate configurations. With the lower diameter and the lower thickness and with the highest diameter and the highest thickness instabilities phenomenon happened during the tests. This is clearly visible in the chart, where the curves have higher oscillations. The irregularities were probably due to poor lubrication and this suggests that proper lubrication is important for a stable control of the process, at least for this material. The ogive being in a steel alloy typically exhibits increased friction problems in the contact with the stainless steel.

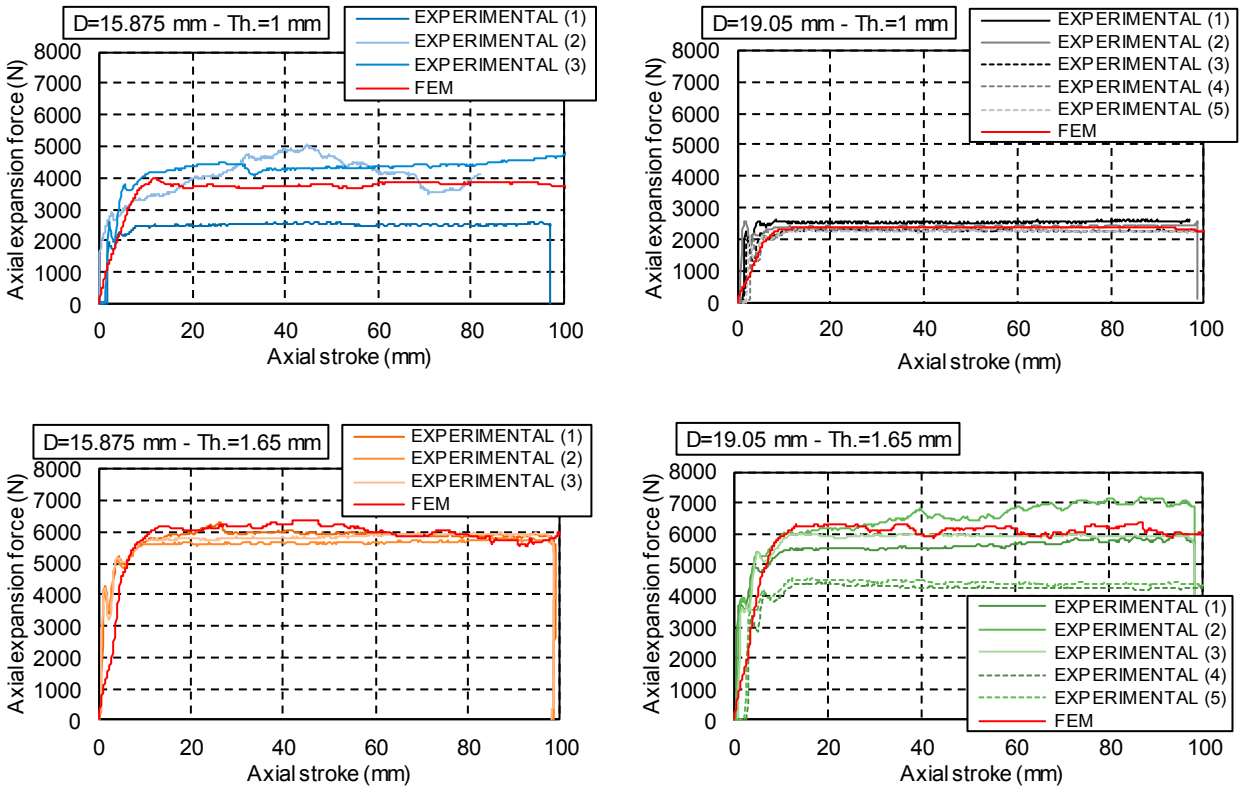

Fig. 7. Experimental tube expansion results in four configurations.

4.4. Titanium ASME SB338, Grade 2 alloy

It is a material of more recent introduction for the examined application, for which the working parameters needed to be identified. To this aim, very few experimental tests were performed with strain-gage measurements applied on the external surface of the tubes. Additionally, in this case only the expansion tests were not performed on specimens for laboratory experiments performed but directly with the equipment used in the industry for the production process of the heat exchangers on longer samples. The tests were in this case much more representative of the actual working conditions but with the drawback of the impossibility to directly measure the insertion force. In this case, the force was estimated on the basis of the measurement of the torque generated by the motor actuating the equipment: this was previously characterized to have a tool to predict the working parameters with simple on-line measurements. However, the estimate is only approximate, and some measure are reported here in Table 2 in terms of the average force during the tube expansion.

The tube characteristics and the working parameters were the same for all tests, namely:

- Thickness, t = 1 mm
- External diameter, d_e = 19.05 mm
- Ogive diameter, d_{ogive} = 17.6 mm
- Interference, i = 0.55 mm

Table 2. Results of the expansion of titanium alloy tubes.

Sample	Average insertion speed (mm/s)	Average torque (N m)	Estimated average insertion force (N)
SB 338Gr2_D19_1_V800_11	52.93	276.0	3997
SB 338Gr2_D19_1_V800_12	52.72	265.6	3847
SB 338Gr2_D19_1_V800_01E	52.77	262.0	3795
SB 338Gr2_D19_1_V800_02E	52.95	262.9	3807
SB 338Gr2_D19_1_V800_03E	53.24	235.2	3405

The average insertion speed was lower than that used with the other materials, this was due to the difficulty to obtain good lubrication during the expansion between the ogive and the inner wall of the tube with the conventional methods. This titanium alloy exhibits good strength characteristics; therefore, the axial expansion force is relatively large. These considerations justify the interest in optimizing the process parameters to control the manufacturing quality and to decrease the energy requested for the operations.

5. Parametric analysis

5.1. Geometry

Obviously, the main affecting parameters are the geometrical characteristics of the tube together with the geometry of the inserted ogive (even if it has been demonstrated by Scattina (2016) that the shape of the ogive has a rather negligible impact). This is also confirmed by the theoretical analysis described by Eq. (2) and (5).

Experimental and numerical tests on the cupronickel tubes clearly illustrate the main influence of the tube thickness (Fig. 8). The points represented in these graphs are the average value estimated with the numerical simulations described in §5.2 or measured during the tube expansion. The thickness appears to have an almost linear influence on the axial expansion force: however, the best approximation is obtained with a parabolic fit. Moreover, the parabolic influence was also predicted by Eq. (5).

The second clear influence is that of the friction coefficient, which is not controllable or easily measurable during the experimental tests. The numerical simulations indicated as the real friction coefficient should have relatively low value, generally not more than 0.10-0.15 as it is clear from the comparison between the numerical simulations and the experimental tests in Fig. 8(a). This topic will be examined in detail in the following section.

To better describe the influence of the thickness, diameter, and interference the Fig. 9 is reported in terms of a normalized axial expansion force evaluated as follows:

$$\frac{F_a}{d_i} = \frac{\pi}{2}\tan(\alpha+\varphi)\left(2+\frac{i}{d_i}\right)\left[S_y\left(\frac{t}{d_i}\right)+E_y\left(\frac{i}{d_i}\right)\frac{\left(\frac{t}{d_i}\right)\left(1+\frac{t}{d_i}\right)}{1+3\left(\frac{t}{d_i}\right)+3\left(\frac{t}{d_i}\right)^2}\right] \tag{6}$$

The two graphs in Fig. 9 show the influence of the thickness over the internal diameter ratio (t / d_i) on the normalized axial expansion and of the interference over the internal diameter ratio (i / d_i). The graphs in Fig. 9 were obtained for the stainless steel tubes with the material properties reported in section §2.

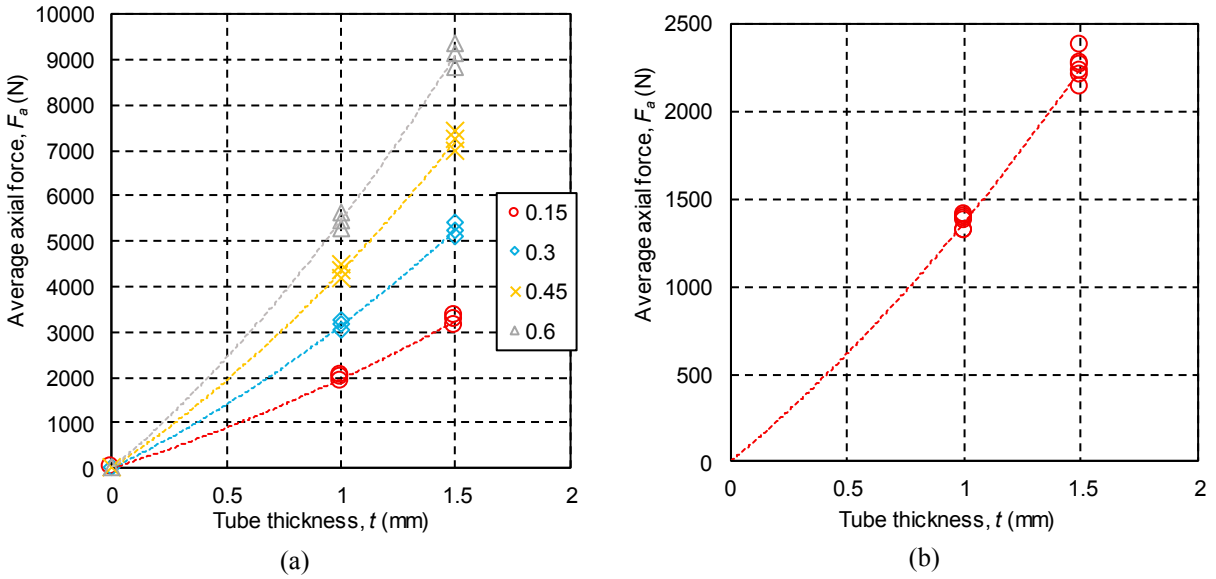

Fig. 8. Effect of the tube thickness on the expansion of the cupronickel tubes: a) numerical results obtained with four different values of the friction coefficient f; b) experimental results.

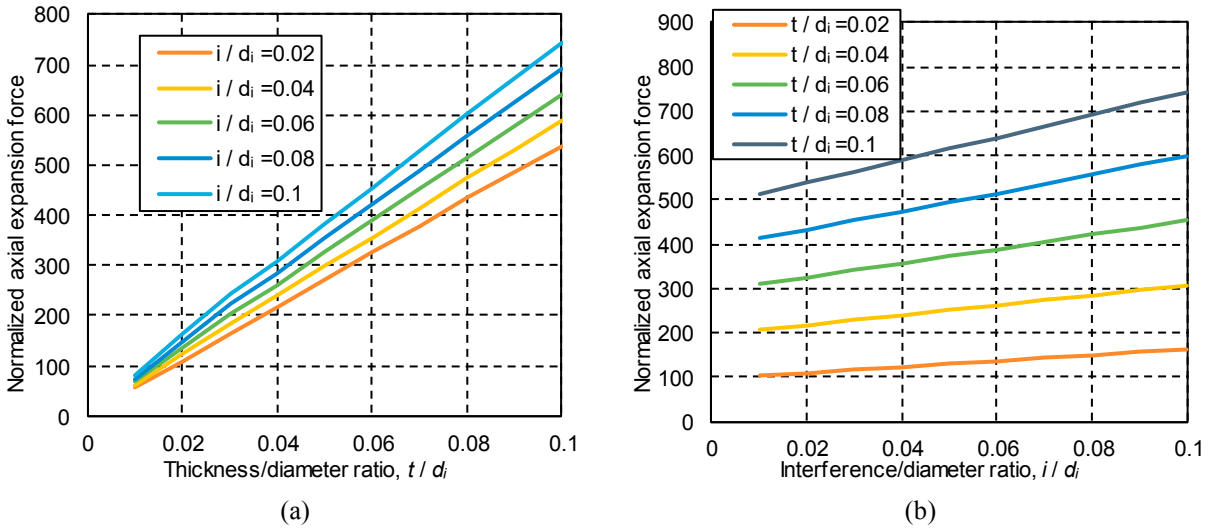

Fig. 9. Effect on the normalized axial expansion force: (a) of the thickness over the internal diameter ratio (t / d_i), and (b) of the interference over the internal diameter ratio (i / d_i).

It appears that both the normalized parameters have an almost linear influence on the normalized force. It can be not obvious that the effect of the interference does not decrease to zero when the interference itself decreases down to zero or near zero. But it should be noted that the force computed by Eq. (6) corresponds to a fully yielded section where a certain interference is required to bring the whole material to plastic flow. An estimate of the minimum interference able to fully yield the section can be obtained with the following expression:

$$\frac{i}{d_i} = \frac{S_y}{E}\left[1-\nu\left(1-\frac{1}{\beta}\right)\right] \tag{7}$$

5.2. Friction

Friction plays a significant role in the evaluation of the axial expansion force. Unfortunately, friction characterization is also quite difficult to obtain: the contact area is not clearly identified, as well as the pressure distribution; the lubrication effect is difficult to be evaluated; the speed and other motion effects cannot be clearly understood.

Finite element analyses carried out with the LS-DYNA 971 solver software, in the implicit version, with a detailed model based on the *MAT_ELASTIC_VISCOPLASTIC_THERMAL material model was used obtaining a good fit with the experimental results (as shown in Fig. 8). The results of the simulations are reported by Avalle et al. (2014), Avalle and Scattina (2012) and Scattina (2016) for the cupronickel alloy. Similarly, satisfactory results were also obtained for the stainless steel as shown in Fig. 7: the red curves are the numerical results.

The analytical model expressed by Eqs. (5) and (6) reflects the experimental observations but the simple contact representation of the expansion process as in Fig. 4 is not at all satisfactory. The contact phenomenon is much more complicated to be described by a simple model where the contact pressure distributed is averaged along the length and radius. However, the model gives good predictions of the axial expansion force if a virtual friction coefficient is obtained: as a matter of fact, this virtual friction coefficient reflects the combined effects of the contact angle α in Fig. 4 and of the friction angle φ. Accepting this hypothesis, the phenomenon is well described in the studied processes. In particular, Fig. 10 compares the experimental results for cupronickel tests with the prediction of the current model: the fit is very good by considering a virtual value of the combined $\alpha + \varphi = 0.78$.

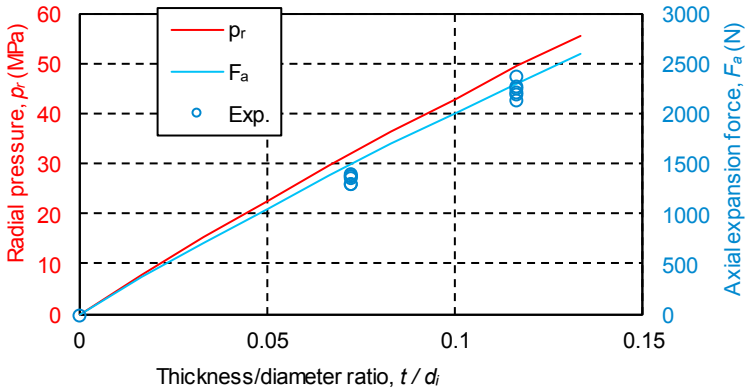

Fig. 10. Comparison of the experimental results (d_e = 15 mm) with the theoretical model prediction in terms of the axial expansion force (cupronickel alloy)

For the stainless steel the comparison is reported in Fig. 11 where the average results for the various tube geometries are compared: due to technological constraints, the combinations of thickness, diameters, and interference were limited and constrained to specific values. The values of the geometrical parameters are reported in the caption of Fig. 11. In this case, the best fit for this complex combination of parameters is obtained with $\alpha + \varphi = 1.36$. Of course, the virtual friction value is much greater than with the cupronickel as expected.

For the titanium alloy, due to the scarcity of experimental results, it is quite difficult to provide an estimate. A reasonable approximation of the average force values from Table 2 is obtained with a virtual friction $\alpha + \varphi = 1.38$.

5.3. Material properties

The analytical model discussed in §3, describes the effect of the material properties in terms of the yield strength S_y of the material of the tube and of the strain hardening modulus E_y. Analysis of the combined effect of these two material properties reveals that the yield strength plays usually the greater role, especially for high yield materials and for smaller interference values: the strain hardening effect depends on the interference whereas the yield is exploited to plastically deform the tube.

For example, in the case of cupronickel, and for the examined combinations of tube geometry and process parameters, the weight of the yield strength and of the strain hardening is almost equal. In the case of the stainless steel the yield strength plays the greater role, it is about 80-85% of the radial pressure and, therefore, of the axial expansion force. In the case of the titanium alloy the yield strength account for almost 90% of the total pressure/force.

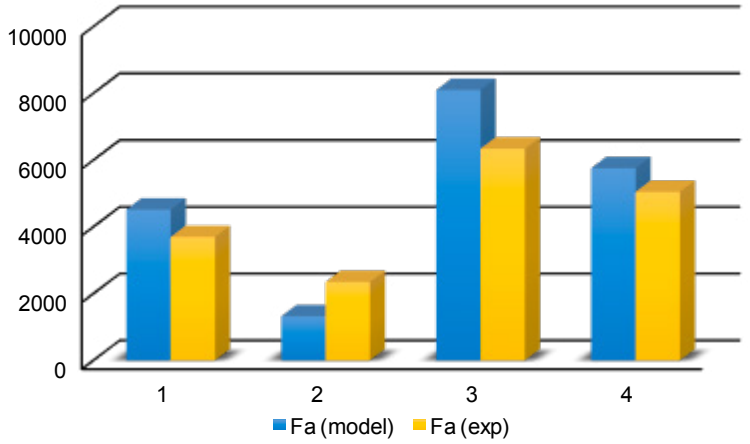

Fig. 11. Comparison of the experimental results with the theoretical model prediction in terms of the axial expansion force for the stainless steel AISI 316. The geometrical configurations in the four cases are: (1) $t = 1$ mm, $d_e = 15.875$ mm, $d_i = 13.875$ mm, $i = 0.725$ mm; (2) $t = 1$ mm, $d_e = 19.05$ mm, $d_i = 17.05$ mm, $i = 0.25$ mm; (3) $t = 1.65$ mm, $d_e = 15.875$ mm, $d_i = 12.575$ mm, $i = 0.775$ mm; (4) $t = 1.65$ mm, $d_e = 19.05$ mm, $d_i = 15.75$ mm, $i = 0.6$ mm.

6. Conclusions

A predictive model of the tube expansion process used in the construction of a class of heat exchangers was described. The model is based on a simplified but sufficient description of the yield process and allows to evaluate the radial pressure exchanged between the tube and the ogive used for the expansion. Moreover, the model can be used to estimate the axial expansion force required for the process. Such a model and its results are extremely important when selecting the process parameters while designing a new product: the process parameters affects technological outputs like the quality and effectiveness of the heat exchanger, and the production costs. Decreasing the process force required to deform the tubes into the fins allows to reduce the required work and, additionally, allows to use smaller machines and lighter components (ogive, push bar, supports, etc.). In previous works of the authors of the current paper, but also of other researchers, numerical models were used obtaining good results in terms of prediction of the process results. An analytical model is simpler and quicker to give a first evaluation for design purposes. The model was validated through the comparison with experimental and numerical results on different materials. In particular, the geometrical and the material parameters are well described. The influence of the friction was more difficult to establish: the conclusion, based on the available results, is that a so called virtual friction value, greater than the physical value, can be used to give good predictions of the axial expansion force. Of course, the virtual friction must be obtained through experimental tests: the reported experiments cover many cases of practical interest, in other cases more experimental tests will be required unless if using rough estimates based on the current experience.

Acknowledgements

The authors acknowledge the financial support of ASTRA Refrigeranti SpA, Alessandria, Italy through several research contracts and the financial support of Regione Piemonte through the *Research Voucher* 2011.

References

Almeida, B.P.P., Alves, M.L., Rosa, P.A.R., Brito, A.G., Martins, P.A.F., 2006. Expansion and reduction of thin-walled tubes using a die: experimental and theoretical investigation. International Journal of Machine Tools & Manufacture 46,1643–1652.

Alves, M.L., Almeida, B.P.P., Rosa, P.A.R., Martins, P.A.F., 2006. End forming of thin-walled tubes. Journal of Materials Processing Technology 177, 183–187.

Avalle, M., Priarone, P.C., Scattina, A., 2014. Experimental and numerical characterization of a mechanicalexpansion process for thin-walled tubes. Journal of Materials Processing Technology 214, 1143-1152.

Avalle, M., Scattina, A., 2012. Sviluppo di una metodologia di simulazione del processo di formatura dei tubi per i fasci tubieri forzati nelle piastre frontali. In: Proceedings of the 41st AIAS (Associazione Italiana per l'Analisi delle Sollecitazioni) National Conference. Padova, Italy, paper #106.

Cowper, G.R., Symonds, P.S., 1957. Strain hardening and strain rate effect in the impact loading of cantilever beams. In: Brown University, Division of Applied Mathematics report 28.

Karrech, A., Seibi, A., 2010. Analytical model for the expansion of tubes under tension. Journal of Materials Processing Technology 210, 356–362.

Li, H.F., Qian, C.F., Yuan, Q.B., 2010. Cracking simulation of a tube sheet under different loadings. Theoretical and Applied Fracture Mechanics 54, 27–36.

Karrech, A., Seibi, A., 2010. Analytical model for the expansion of tubes under tension. Journal of Materials Processing Technology 210, 356-362.

LS-DYNA Keyword User's Manual, version 971, 2007. Livermore Software Technology Corporation (LSTC), Livermore, California 94551.

Madhusudana, C., Cheng, W.-W., 2007. Decrease in thermal contact conductance and the contact pressure of finned-tube heat exchangers assembled with different size bullets. Journal of Heat Transfer 129, 907–911.

Nadai, A., 1950. Theory of Flow and Fracture of Solids, 2nd ed. McGraw-Hill Book Company Inc., New York.

Scattina, A., 2016. Numerical analysis of tube expansion process for heat exchangers production. International Journal of Mechanical Sciences 18, 268-282.

Schlünder, E.U. (Ed.-in-Chief), 1983. Heat Exchanger Theory. Hemisphere Publishing Corporation, Düsseldorf

Seibi, A.C., Barsoum, I., Molki, A., 2011. Experimental and numerical study of expanded aluminum and steel tubes. Procedia Engineering 10, 3049–3055.

Tang, D., Li, D., Peng, Y., 2011. Optimization to the tube–fin contact status of the tube expansion process. Journal of Materials Processing Technology 211, 573–577.

Tang, D., Li, D., Peng, Y., Du, Z., 2011. Mechanical Expansion of Thick-Walled Microgroove Tube for High Pressure ACR System. Journal of Pressure Vessel Technology 133, paper #021202.

Tang, D., Peng, Y., Li, D., 2008. An experimental and numerical study of the expansion forming of a thick-walled microgroove tube. Proceedings of the Institution of Mechanical Engineers Part C: Journal of Mechanical Engineering Science 223,689.

Tang, D., Peng, Y., Li, D., 2009. Numerical and experimental study on expansion forming of inner grooved tube. Journal of Materials Processing Technology 209, 4668–4674.

Thulukkanam, K., 2000. Heat Exchanger Design Handbook. CRC Press.

Yang, J., Luo, M., Hua, Y., Lu, G., 2010, Energy absorption of expansion tubes using a conical–cylindrical die: Experiments and numerical simulation, International Journal of Mechanical Science 52, 716–725.